Article:
Xu, N, Wang, C, Yang, L et al. (2022) Probing the Tribochemical Impact on Wear Rate Dynamics of Hydrogenated Amorphous Carbon via Raman-Based Profilometry. ACS Applied Materials and Interfaces, 14 (1). pp. 2071-2081. ISSN: 1944-8244

https://doi.org/10.1021/acsami.1c21824

Probing the tribochemical impact on wear rate dynamics of hydrogenated amorphous carbon via Raman-based profilometry

Nan Xu,[*,†] Chun Wang, [†] Liuquan Yang,[†] Gin Jose,[‡] and Ardian Morina [*,†]

[†] Institute of Functional Surfaces, School of Mechanical Engineering, University of Leeds, Leeds LS2 9JT, United Kingdom

[‡] School of Chemical and Process Engineering, University of Leeds, Leeds LS2 9JT, United Kingdom

ABSTRACT: Solid-liquid lubricating system has received significant attention as a promising way for energy savings and emission control. For deeply understanding their tribological behaviours, it is necessary to study interaction mechanisms between solid and liquid lubricants from tribochemical viewpoint, as tribofilms formed by tribochemical products on contact surfaces critically affect whole tribological process. Continually or periodically monitoring tribofilm formation and evolution can contribute significantly to clarifying its dominating role on tribological behavior under boundary lubrication. However, detecting tribofilm in situ remains a big challenge for conventional surface analytical approaches, mainly due to their limitations in accessing tribofilms or low signal intensities of thin tribofilms. In this study, a highly sensitive Raman-based profilometry with in-situ potential has been developed for detecting molybdenum dialkyldithiocarbamate (MoDTC)-derived tribofilms and exploring their effect on a-C:H wear over time. The optical properties of tribochemical products formed on coating surface in different wear-stages could result in extra attenuation of Raman signal intensities, in the form of measurement deviations in wear depth. By monitoring the deviations, key information of tribofilm compositions was obtained

and a two-stage wear progression mechanism was proposed for the first time to clarify the detrimental effect of MoDTC-derived tribofilm on a-C:H wear by combining detailed structure and composition analysis.

KEYWORDS: Raman spectroscopy; tribochemistry; diamond-like carbon; solid-liquid lubricant; wear measurement.

1. INTRODUCTION

As a promising way for energy savings and emission control, combination of solid and liquid lubricants in the tribological systems have attracted considerable research attentions in diverse engineering fields, including lightweight design, manufacturing, aeronautics, marine equipment, automobiles [1-6]. This approach can effectively integrate the advantages of solid and liquid lubricants while minimizing their individual drawbacks through interaction [1]. To meet the requirements of increasingly demanding lubricating conditions in the future, it is therefore necessary to develop novel solid-liquid composite lubricating systems. Considering most of the existing liquid lubricants are tailored for ferrous-base surfaces [4], in-depth studies of the interaction between non-ferrous surfaces and liquid lubricants are therefore essential for developing high-performance lubricating systems and understanding further mechanisms, such as tribochemical reactions on coating surfaces under additive-lubricated conditions.

To date, the majority of experimental studies on friction and wear mechanisms of boundary lubricated systems are mainly based on understanding the tribofilm nature (e.g. chemical composition, structure, and mechanical properties) and their tribochemical interaction with contact surfaces [7-9]. In the case of MoDTC, they have been widely employed in engine oils as a classic friction modifier (FM) which decomposes into molybdenum disulphide (MoS_2) sheets and molybdenum trioxide (MoO_3) under the action of friction forces [4]. For ferrous-base contact surfaces, its effectiveness in friction-reduction can be attributed to the formation of tribofilms, containing nano-MoS_2 sheets with layer-lattice

structure and weak interlaminar shear forces [10]. However, when applying MoDTC-containing oil on the steel/DLC contacts, it dramatically accelerated the wear rate of DLC, further triggering coating failure [11-16]. It is well accepted that MoDTC-derived tribochemical products play a critical role in this detrimental effect. The wear acceleration mechanisms of MoDTC on DLC surfaces in previous studies can be summarized as follows: i, oxidation-reduction reaction between DLC and molybdenum oxides [16]; ii, abrasive wear of molybdenum oxides [4]; iii, abrasive wear of molybdenum carbides formed via tribochemical reaction [15]; iv, re-hybridization of C-C bonding from sp^3 to sp^2 under severe tribological conditions and delamination of this sp^2-rich carbon layer [14]. It should be also pointed that some of the above mechanisms (e.g. abrasive wear mechanism of molybdenum oxides and re-hybridization mechanism of C-C bonding) remain controversial [13]. More importantly, it is still unclear which type of tribochemical products dominates the coating wear behavior in different wear-stages when lubricated with MoDTC.

To reveal the impact of tribochemical products, various surface analytical techniques have been applied to identify the composition and microstructure of MoDTC-derived tribofilms [4, 14-16]. Although a significant progress has been achieved in understanding the chemical nature of tribofilms, the wear acceleration mechanisms are still not fully understanded. The main reason is the difficulty in continuously or periodically obtaining the tribofilm composition during the wear process. It is well-known that wear process is always accompanied with the formation and evolution of tribochemical products. In different wear-stages, there exists specific tribochemical products dominating the tribological behavior. It is therefore of great importance to verify the tribofilm composition in the correlated wear-stage. However, this remains a significant challenge for conventional surface analytical approaches due to their limitations in accessing the tribofilms in friction process or low signal intensities of thin tribofilms with nanometers thickness [7].

Raman spectroscopy, as a powerful surface analysis technique, has been widely used in chemical analysis of tribofilm formation and removal [15,17-19]. By combining a flexible sampling arm, in-situ chemical analysis of MoDTC-derived tribofilm has been realized by combing Raman spectroscopy and in-situ tribometer [19]. With development of highly compact laser excitation and detection system expected in near future, Raman spectroscopy displays considerable promise for continuously monitoring the wear process of mechanical components. One main limitation posed by applying Raman spectroscopy in in-situ monitoring is the low Raman intensities of thin tribofilms. As indicated in this study, Raman peaks, attributed to MoDTC-derived MoS_2 nanosheet, cannot be detected for MoS_2 with small crystal size or poor crystallinity. To overcome this limitation, a highly sensitive Raman-based profilometry was introduced in this study. This new approach employs a silicon layer with high Raman intensity under the target coatings (a-C:H) to provide information on the coating wear and tribofilm formed on the coating surfaces. The formation of additive-derived tribofilms caused extra attenuation of Raman signal which led to remarkable deviations of coating thickness measurement via Raman-based approach. Meanwhile, tribofilms formed by different tribochemical products displayed varying degrees of attenuation for Raman signal due to their distinct optical properties. Therefore, critical information about tribofilm composition and evolution could be obtained by monitoring the deviation variation, which contributed significantly to the clarification of coating wear mechanisms under additive-lubricated condition. To verify the Raman-based approach, structural and composition analysis of tribofilms were also performed by combination of Raman, TEM (transmission electron microscopy), FIB (focused ion beam) and FFT (fast Fourier transform) patterns. This proposed methodology has the potential to open a new pathway for in-situ detecting tribofilms, which is crucial for revealing coating wear mechanisms and developing novel solid-liquid composite lubricating systems.

2. EXPERIMENTAL SECTION

2.1. Synthesis of hydrogenated amorphous carbon films (a-C:H). The a-C:H films were deposited by a Plasma Enhanced Chemical Vapour Deposition technique (PECVD) with acetylene as gas feed (Flexicoat 850, Hauzer Corp., Netherlands). Two kinds of substrates, n-type silicon (100) wafers (10 mm × 10 mm × 0.5 mm, Ra < 1 nm) and glass plates (25 mm × 25 mm × 1 mm, Ra < 1 nm), were employed. The a-C:H films deposited on silicon wafers were used for tribo-test, thickness quantification, and characterization of structure and composition, while that on glass plates was for the optical studies of a-C:H films. The substrates were ultrasonically cleaned by acetone and ethanol. Before the deposition, the vacuum chamber was evacuated to a base pressure of 3.0×10^{-3} Pa and heated to 200 °C. After that, the substrate surface was etched in argon plasma at the pressure of 0.15 Pa for 5 mins and roughness was ca. 6.1 nm (*R*a). During the deposition, a pulsed DC power with bias voltage at -500 V was applied to the substrates and the chamber pressure was 0.85 Pa with acetylene as feeding gas with feeding rate at ca. 250 sccm. The deposition time of the a-C:H films with thickness of ~ 183 and 277 nm was 100 mins and 130 mins, respectively. Additionally, part of silicon wafer was sheltered for measuring the thickness of a-C:H films by NPFLEX 3D non-contact optical profilometer, schematically shown in Figure S1. Detailed information of a-C:H film is as follows: hydrogen content of ca. 22 %, hardness of ca. 21 GPa, Young's modulus of ca. 180 GPa, initial roughness of ca. 5.3 nm (*R*a) and Poisson's ration of 0.2.

2.2. Tribological experiments. The friction experiments were conducted via a ball-on-disc tribometer (Bruker UMT-Tribolab) at room temperature under both dry and oil-lubricated condition. The samples with a-C:H film deposited on silicon wafer was clamped on a reciprocating platform, meanwhile employing a fixed upper ball (AISI 52100 steel, 6.35 mm in diameter, HRC 60-67) as the counterpart. In oil-lubricated condition, PAO4 with 0.8 wt.%

MoDTC (molybdenum dialkyldithiocarbamate) was employed as lubricant. Dry tribo-test conditions: a-C:H of 277 nm thickness on silicon wafer, time of 30 to 110 mins, applied load of 1N (580 MPa), frequency of 10 mm/s, ambient environment. Oil-lubricated test conditions: a-C:H of 183 nm thickness on silicon wafer, PAO with 0.8 wt.% MoDTC, time of 30 to 140 mins, applied load of 1N and 10 to 40 N (1.2 to 2.0 GPa), frequency of 10 mm/s, ambient environment.

2.3. Materials Characterization. A Renishaw inVia^{TM} Raman spectrometer was used to quantify the thickness of a-C:H films in line-scanning mode and backscattering geometry with 488 nm laser and 1mW laser power. As indicated in section 2.1, the silicon wafers were etched in argon plasma before depositing a-C:H. Considering the effect of etching process to the Raman signal of silicon wafer, a standard silicon wafer was etched in the same condition and tested first to obtain the Raman intensity of silicon without attenuation ($I_o\beta$) before every Raman line-scanning test. NPFLEX 3D non-contact optical profilometer and TALYSURF 120L contact profilometer were employed to characterize the wear scars and verify the results of Raman-based coating wear quantification method. UV-vis-NIR spectroscopy (PerkinElmer Lambda 950) was employed to study the optical properties of a-C:H films deposited on glass plates.

A focused ion beam (FIB, FEI Helios G4 CX DualBeam FIB-SEM) was used to prepare thin cross-sectional lamellar specimens of tribofilms for TEM (transmission electron microscopy) investigations. Prior to FIB milling, the contact area was coated by a layer of iridium (20 nm) to eliminate contaminations. Then, the samples were transferred into FIB-SEM chamber and coated by a thick Pt film (~ 1 μm) in order to protect coating structure during FIB milling (low-kV Ga^+ ion milling). FEI Titan3 Themis 300 TEM/STEM (Scanning transmission electron microscopy) equipped with Gatan Quantum ER energy filter and

energy dispersive X-ray spectroscopy (EDS) was employed for TEM characterization and elemental mapping.

3. RESULTS AND DISCUSSION

3.1. Improved profilometry for coating wear measurement

To obtain accurate topographic information of wear scars, both non-contact optical and contact profilometers were employed to characterize the tribo-tested samples as shown in Figure 1 and S2. Figure 1a shows the morphologies of the wear tracks under test time of 30 mins. Through comparison, the wear profiles obtained by different profilometers show similar depth evolution trend along the wear scar. However, when the test time was extended to 60 mins (Figure 1b), the wear profile given by non-contact optical profilometer displayed obvious depth rising in the centre area, which was not observed in the result of contact profilometer. It is well known that non-contact optical profilometer builds up a 3D map by collecting array signals of light interference of reflected light. Given the high sensitivity towards optical signal, it is suggested that the tribo-induced variation of optical properties (i.e., reflectivity) on the top surface, termed tribo-induced polishing effect, may affect the intensity of light signal and further results in remarkable measurement deviation of optical profilometer.

To avoid the influence of tribo-induced polishing effect on the measurement accuracy of optical profilometer, an optical signal synchronization layer of iridium with uniform thickness (~ 20 nm in Figure S3) was deposited on the tribo-tested sample by DC magnetron sputtering to provide a top surface with consistent optical properties. Then, optical profilometer was used again to characterize the sample and it was found that the depth rising in the centre area disappeared after depositing iridium layer and the wear profile showed similar evolution trend with that of contact profilometer. Similar tribo-induced effect was also observed for tribo-tested samples with test time of 90 and 110 mins in Figure S2. This

improved profilometry with optical signal synchronization layer of iridium was used to provide accurate wear depth as standard reference to verify the quantified results based on Raman signal in the later section.

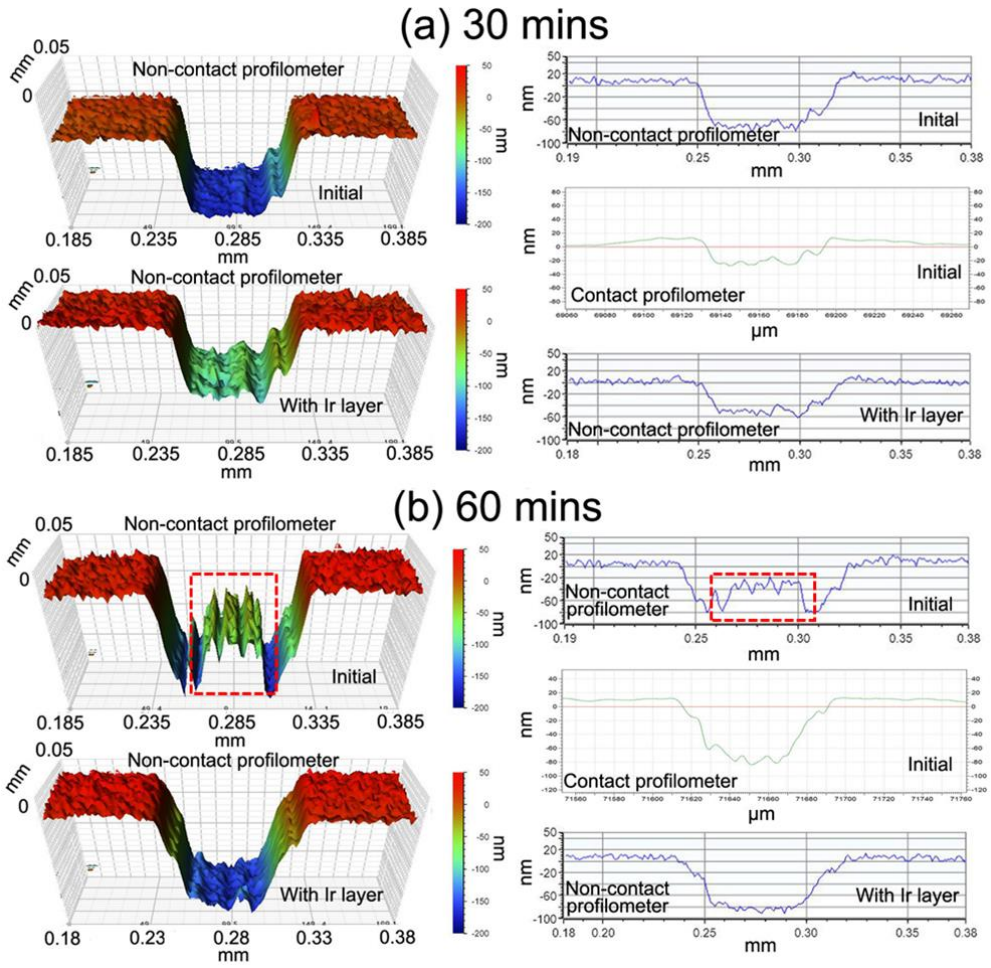

Figure 1. Comparison of wear profile curves obtained by non-contact optical profilometer (before and after depositing iridium layer on top of a-C:H) and contact profilometer for tribo-tested samples under dry friction (a, 1N, 30mins; b, 1N, 60mins). The marked areas in (b) indicate the measurement deviations of optical profilometer (before depositing iridium layers).

3.2. Raman-based profilometry for tribofilm detection

In our previous study [20], an accurate Raman-based coating thickness quantification method was established by introducing a silicon layer with strong Raman signal under the target coatings of a-C:H. As shown in Figure S4, the Raman signal intensity of silicon underlayer will be attenuated in the a-C:H due to absorption and reflection. Based on Beer's law [21], the

relationship between thickness of a-C:H and Raman intensity of attenuated silicon signal was constructed by equation (5) in S1.1 section. It has also been demonstrated that the Raman intensity of silicon decreased logarithmically with increasing the a-C:H thickness. Detailed information of Raman-based coating thickness quantification process can be found in S1.1 section and our previous study[20].

In this study, this proposed approach was employed to detect the formation and evolution of additive-derived tribofilm on the coating surface in the tribological process. As shown in Figure 2, the formation of tribofilms, composed of tribochemical products, on the coating surface can result in extra attenuation of Raman signal from silicon underlayer, further leading to measurement deviation of Raman-based coating thickness measurement. Considering the distinct optical properties of tribochemical products, key information of tribofilm compositions can be obtained by monitoring the measurement deviation.

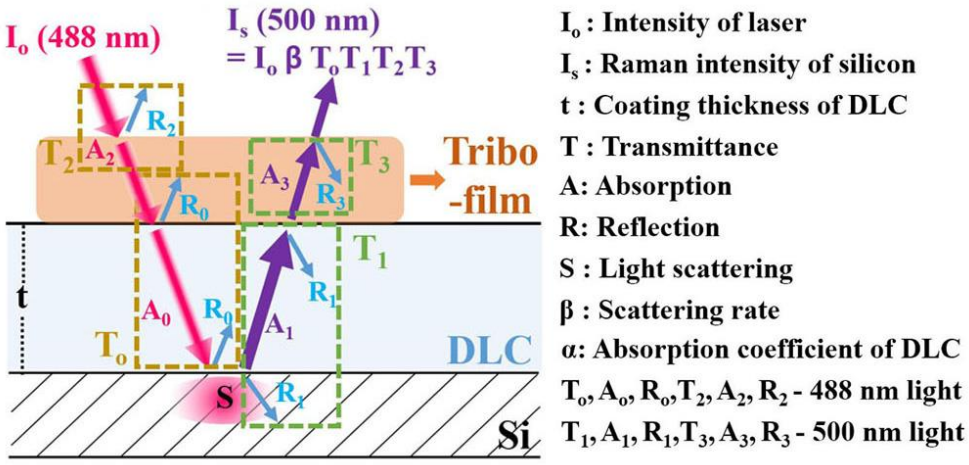

Figure 2. Schematic illustration of Raman-based coating thickness quantification process with additive-derived tribofilms on coating surface.

3.3. Wear behavior of a-C:H under additive-lubricated condition

For gaining fundamental insights into wear behavior of a-C:H coatings under additive-lubricated condition, this proposed Raman-based method was employed to study effect of MoDTC-derived tribofilms on the wear behaviors a-C:H coatings. As shown in Figure S7, a series of tribo-tests were performed on the a-C:H/steel contact.

After removing the oil, Raman-based approach was first used to quantify the wear depth via the same process as stated in the last section. Then improved optical profilometry (with iridium layer on top) was employed to characterize the wear scars to provide standard reference. Compared with the standard reference, obvious depth deviations obtained by Raman-based method (presented as black bars) were observed in Figure 3. It is well-accepted that MoDTC tribofilm, composed of various tribo-chemical products, could be formed on the sliding surface of a-C:H [22-27]. Since they possess different optical properties compared with a-C:H, obvious deviations of Raman-based method were obtained. The depth difference between the results of optical profilometer with and without iridium layers also confirms the formation of tribofilms with different optical properties. Table 1 summarizes the optical properties of MoDTC-derived tribochemical products [28-35]. Based on equation (3) and (4) in S1.1 section, it can be suggested that tribofilms should be composed of products with lower transmittance than a-C:H, since decreasing the transmittance resulted in the reduction of Raman signal intensity which corresponds to the thickening of coating in the form of depth decrease. As shown in Table 1, MoS_2, MoC, and Fe_3O_4 possessed lower transmittance (higher absorption coefficient or/and reflectivity) than a-C:H coating. Based on Raman spectra in Figure 3f, it can be suggested that MoS_2 and MoC should be the main tribo-chemical products of MoDTC. Raman signals of MoS_2 and MoC could be detected on a small number of deviation points as marked in the Figure 3. This should be attributed to the low Raman intensity of small crystal size or poor crystallinity of MoS_2 and MoC formed on other deviation points. However, as quantified wear depth based on Raman scattering signals depended on the transmittance of top coatings, this Raman-based approach could provide insight into tribofilm formation and evolution on the top sliding surface based on the measurement deviations.

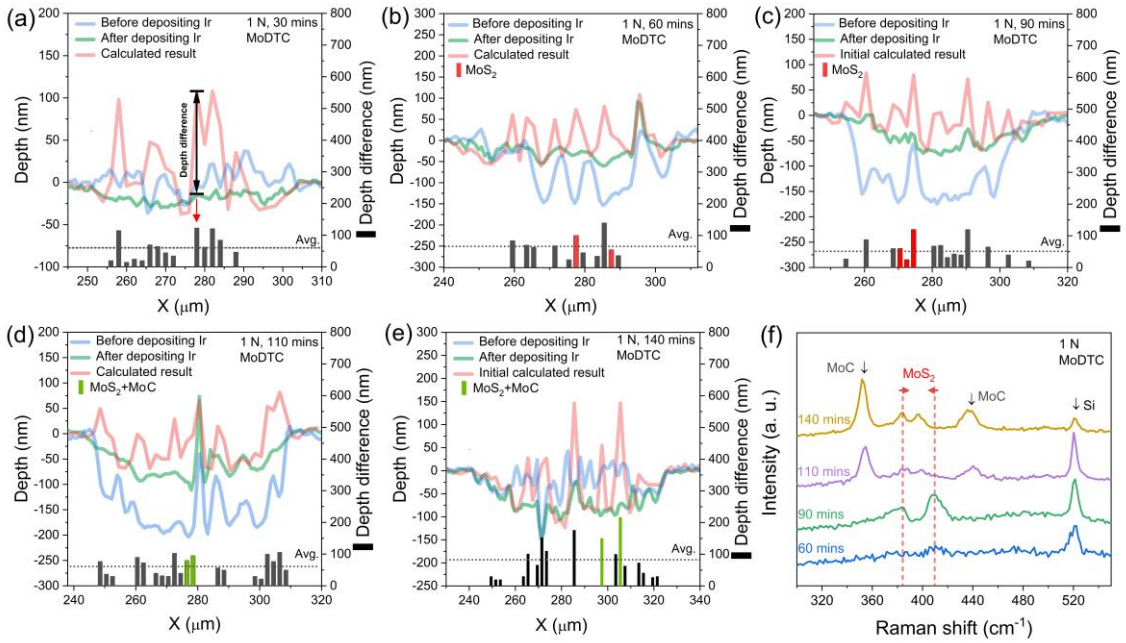

Figure 3. (a)-(e) Comparison between calculated wear profiles derived from Raman intensity of silicon bands and wear profiles characterized by non-contact optical profilometer (before and after depositing iridium layer on top of a-C:H) under oil lubrication (PAO with 0.8 wt.% MoDTC, test time of 30-140 mins, applied load of 1 N). Black bars display the depth deviation of wear depth values obtained between Raman-based method and non-contact optical profilometer (after depositing iridium layer). Red and green bars indicate the formation of MoS_2 and MoS_2 + MoC, respectively. (f) Raman spectra of MoS_2 and MoS_2+MoC detected on the tribo-tested samples under different test time.

Table 1. Reflectivity (R) and absorption coefficient (α) of MoDTC-derived products in the wavelength region 450-550 nm reported in the literature.

Materials	R (%)	α(cm^{-1})
MoO_3 [28,29]	~ 20	~ 4×10^4
Fe_2O_3 [30,31]	~ 10	~ 5×10^4
MoC [32, 33]	~ 50	~ 12×10^4
MoS_2 [34, 35]	~ 19	~ 15×10^4

As shown in Figure 3f, when test time was less than 90 mins only MoS_2 was detected, and MoC always appeared simultaneously with MoS_2 in the longer test time. Meanwhile, the blue shift of the E^1_{2g} vibration and red shift of A_{1g} vibration of MoS_2 in the Raman spectra with the formation of both MoC and MoS_2 indicated the degradation of MoS_2 crystal [36]. It was

therefore suggested that MoS_2 crystals were gradually converted into MoC in friction process. Thermal carburization of MoS_2 into MoC has been reported in the literature [37], where MoS_2 shell was broken first through reaction between hydrogen and sulfur atoms of MoS_2, followed by CH_4 attack to form MoC. Therefore, the key reaction conditions for MoS_2 carburization were heat, active sites on MoS_2 resulting from structure degradation as well as carbon source. Indeed, these requirements can also be fulfilled in friction process: (a) Tribo-contact imposed shear forces on the coating can be partly dissipated as heat. Meanwhile, tribo-induced shear stress can result in the activation energy reduction of chemical reactions, leading to the decrease of reaction temperature [38]. (b) Tribo-induced transformation or degradation of the microstructure of nano-additives can also be realized in friction process [39-41]. (c) Some studies have demonstrated the degradation of lubricating oil into shorter chains in the friction process, which could further form solid carbon-based films [8,9,42,43]. While for PAO oil used in this study, the degradation of olefin chains into shorter hydrocarbon fragments was also found under the action of friction forces [8,42]. Additionally, CH_4 and H_2 have been demonstrated as the main products of tribo-chemical degradation from PECVD a-C:H coatings [44].

For further verifying the finding of MoS_2 and MoC formation from MoDTC, FIB with in-situ lift-out technique was used to fabricate cross-sectional lamellar specimens of tribofilms for structure and composition characterization by TEM and FFT. As shown in Figure 4a, a thin tribofilm (thickness below 10 nm) with small patches of MoS_2 sheets was formed under 30 mins test time. The distance between MoS_2 layers was measured to be 0.62 nm, agreeing with the lattice structure of MoS_2 [37]. When prolonging test time to 90 mins (Figure 4b), significant increase of tribofilm thickness (up to ~ 35 nm) was observed with the formation of highly crystallized MoS_2 structures (~ 3-4 layers). With extending the time to 140 mins, the formation of hybrid structures of nano-MoS_2 and nano-MoC was confirmed by TEM images and FFT patterns. The interplanar crystal spacing and intersection angle agreed very well

with those of (200) and (111) planes of cubic α-MoC (Figure 4c-II and III) [45,46]. It was demonstrated that MoS_2 was formed in the initial stage and further converted to MoC.

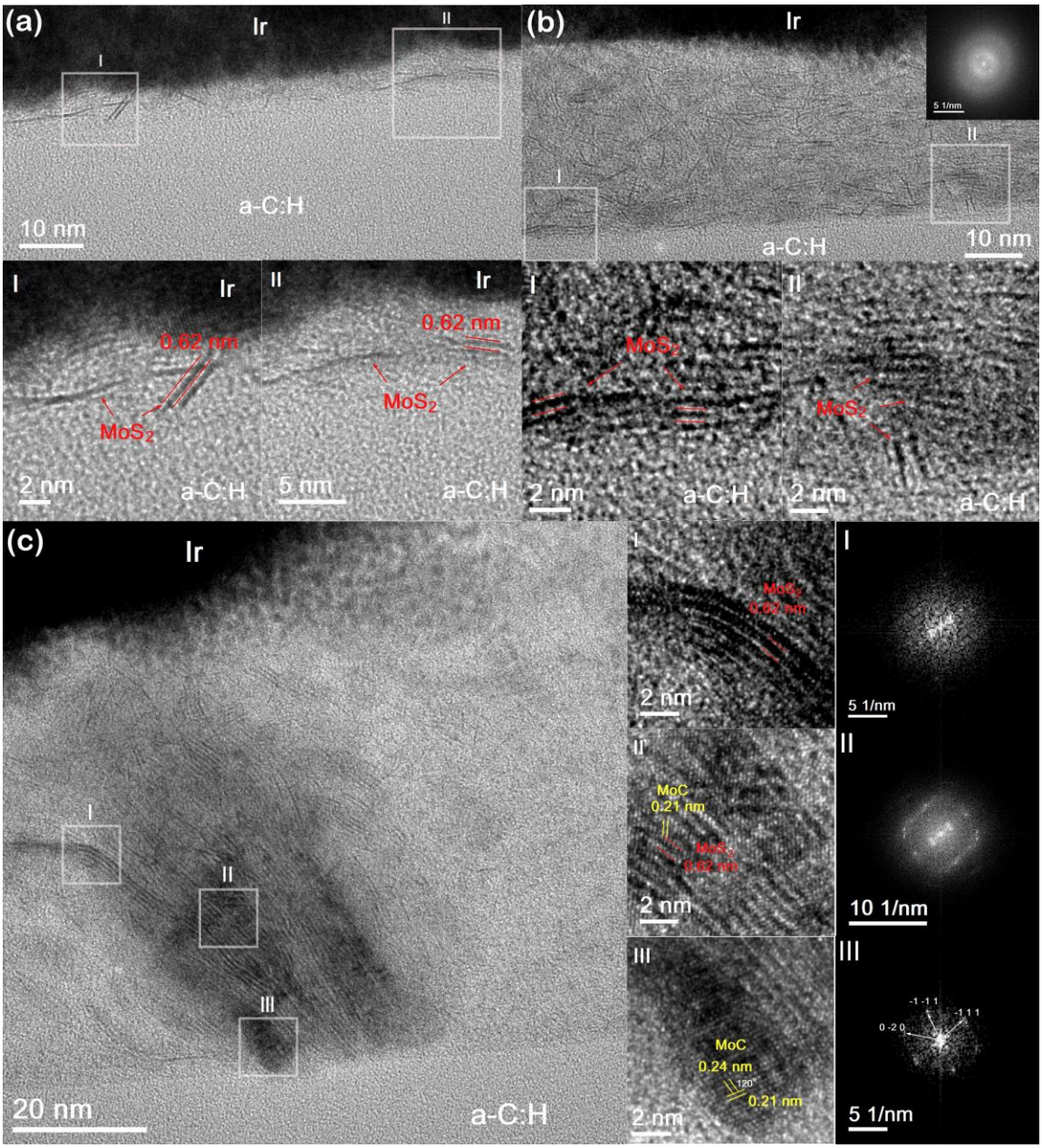

Figure 4. HRTEM images showing the tribofilms formed under different test time (a, 30mins; b, 90mins; c, 140 mins) and fast Fourier transform (FFT) patterns clarifying the crystal phases.

Figure S8 shows the evolution of maximum width and depth of wear scars with test time. It was found that the width increased linearly while depth trend could be divided in two stages. Compared with stage 1, the growth rate of wear depth in stage 2 was obviously increased, indicating a higher wear rate. For better understanding the underlying mechanism, average

values of depth difference between the results of Raman-based wear measurement and improved profilometry was given in Figure S8. As the depth difference was attributed to the formation of tribofilm with different optical properties on the top surface of a-C:H, it could provide valuable information about the tribofilm formation and evolution. Here the average depth difference increased remarkably in the stage 2 in contrast with stage 1, indicating the formation of tribo-chemical products with lower transmittance. This agreed with the above finding about carburization of MoS_2 into MoC under the longer tribotest time, as MoC displayed lower transmittance (higher reflectivity) than MoS_2 as shown Table 1. Meanwhile, MoC can trigger abrasive wear and speed up coating wear due to its high hardness [16]. As suggested above, the shear forces critically promoted the carburization of MoS_2 into MoC in the friction process. To further validate this hypothesis, wear behaviors of a-C:H lubricated by MoDTC-containing oil under high applied load (10-40 N) were investigated as shown in Figure 5. Similarly, the wear rate was accelerated dramatically in stage 2 accompanied by the formation of abundant MoC (Figure 5d), indicating the critical role of MoC in wear acceleration of a-C:H films in the stage 2.

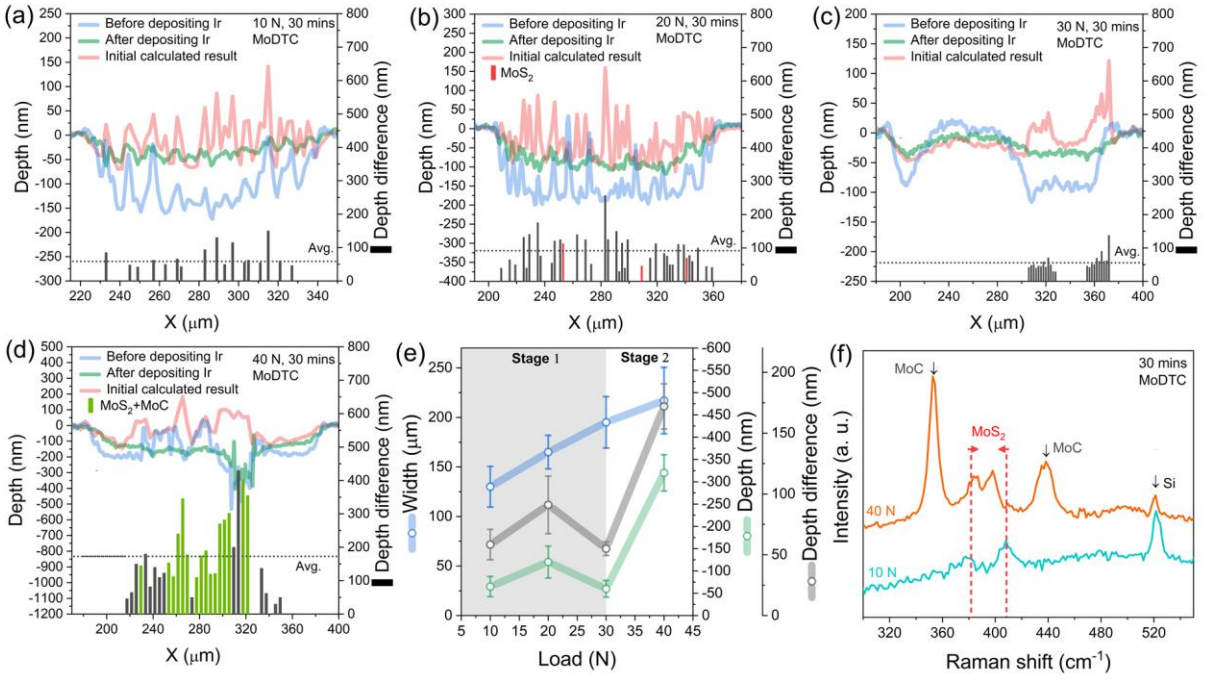

Figure 5. (a)-(d) Comparison between calculated wear profile derived from Raman intensity of silicon bands and wear profile characterized by non-contact optical profilometer (before and after depositing iridium layer on top of a-C:H) under oil lubrication (PAO with 0.8 wt.% MoDTC, test time of 30 mins, applied load of 10-40 N). Black bars displayed the depth difference of wear profile curves obtained by Raman-based method and non-contact optical profilometer (after depositing iridium layer). Red and green bars indicated the formation of MoS_2 and MoS_2 + MoC, respectively. (e) Evolution of width, depth and average depth difference of wear scars with load. (f) Raman spectra of MoS_2 and MoS_2+MoC detected on the tribo-tested samples under different test time.

As indicated in the introduction, the effect of MoDTC on the wear acceleration of a-C:H film on the steel/ a-C:H contact under ambient environment has become one research hotspot during the past decade. It is well accepted that MoDTC-derived tribochemical products play a key role in this detrimental effect. However, the mechanisms about which type of products dominates the wear process are still not fully understood. In this study, for the first time it is reported that the wear behavior of a-C:H coatings with MoDTC as lubricating additive accelerates during the test in contrast to the condition lubricated by pure PAO [20]. Based on the above results, a two-stage wear process was proposed to explain the wear acceleration mechanism as shown in Figure 6. It is well accepted that MoS_2 is always formed accompanied by MoO_3 formation [24]. It is suggested that wear acceleration in the first stage can be attributed to the catalytic effect of molybdenum oxides in the oxidation of a-C:H coating and easy-shear capability of top oxidation layers [47-49]. Due to the easy-shear capability of oxidation products [47,50-54], only tiny oxidation layer remains on the surface with the thickness around several nanometers [51]. Considering the large probe depth of Raman (~300 nm) and its high sensitivity towards sp^2-C phase, the bulk signal of a-C:H dominates the Raman spectra, explaining why we cannot detect the oxidation layer by Raman spectroscopy which is in line with the literature [16,23,51]. Meanwhile, to clarify the formation of MoO_3 in tribofilm, TEM and EDS elemental mapping were used to characterize the

composition and structure of tribofilm as shown in Figure 7. Figure 7a shows the HRTEM image of tribofilm formed after tribo-test (1 N, 90 mins). In the selected area, obvious accumulation zones of highly crystalline MoS_2 are observed, which are surrounded by material with amorphous structure. By comparing the EDS mapping images of Mo, S and O, it is found that elements Mo and O are enriched in the areas of amorphous material, while the MoS_2 accumulation areas are abundant in Mo and S. This finding gives direct evidence of MoO_3 formation in the tribofilm and its accompanying relationship with MoS_2. In addition, the main reason why it is hard to detected MoO_3 via Raman is due to low Raman intensity of the poor crystalline MoO_3 in the tribofilm. Meanwhile, the formation of MoDTC-derived MoO_3 in the tribological process has also been confirmed based on the XPS analysis in the literature [4,16,24,27]. While for the second wear stage, the tribo-induced shear forces trigger the degradation of PAO into hydrocarbon fragments (carbon source) and generate heat for prompting the conversion of MoS_2 into MoC. Due to its high hardness, MoC acts like abrasive particle to further accelerate the wear of a-C:H in the second stage.

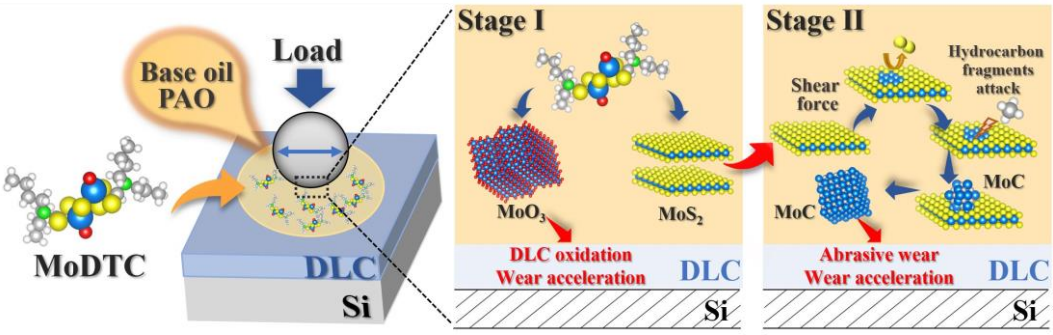

Figure 6. Schematic illustration of the two-stage wear process for clarifying the wear acceleration mechanisms of a-C:H films under MoDTC-lubricated condition.

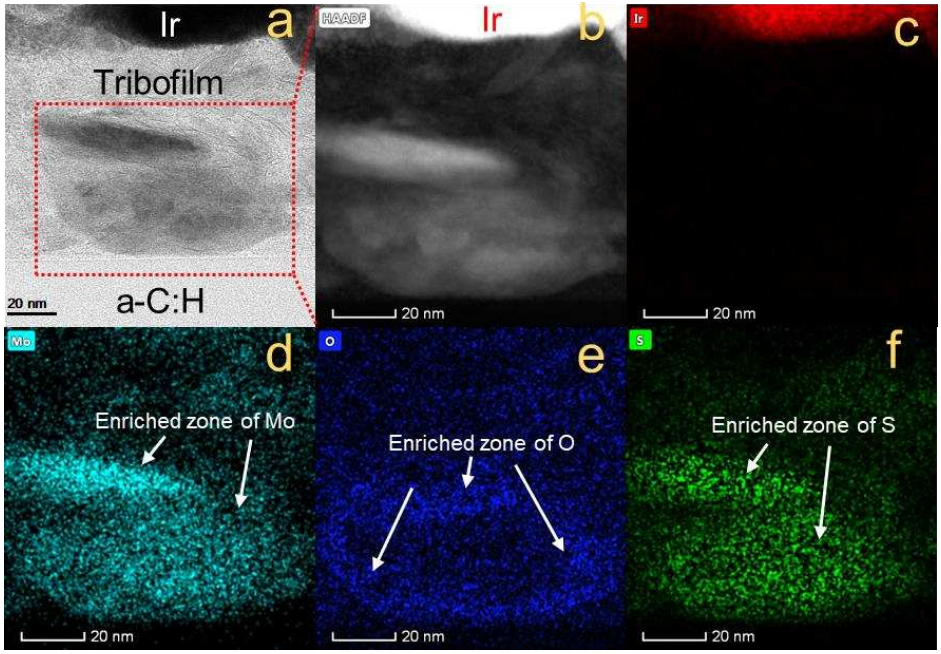

Figure 7. (a) HRTEM image showing the tribofilms after tribo-test (1 N, 90 mins). (b) High-angle annular dark-field (HAADF) image of selected area in (a). (c-f) The corresponding EDXS elemental mapping images of Ir, Mo, O and S.

To further verify this wear mechanism, EDS was employed to characterize the element distribution in the interface area between a-C:H and tribofilm as displayed in Figure 8. Figure 8a shows the HRTEM image of tribofilm after tribo-test (1 N, 140 mins) where hybrid structure of nano-MoS2 and nano-MoC is observed as stated above. EDS line-scanning was conducted from the bottom of hybrid structure to a-C:H as shown in Figure 8b and the corresponding result is given in Figure 8c. Along the line-scanning direction, the C concentration increases continuously and achieved maximum value when it is close to the a-C:H surface, while the concentrations of Mo and S show opposite trend and drop to zero when it reaches the a-C:H surface. An interesting finding is the oxygen doping region in the subsurface of a-C:H (thickness of ca. 3 nm, grey area in Figure 8c), which directly demonstrates the catalytic effect of MoO_3 on a-C:H surface under shear forces leading to significant weakening and wear of a-C:H. In addition, the accelerated wear in the second stage is caused by the abrasive wear of hard MoC rather than the reason of sulphur doping in

the subsurface area of DLC reported in the literature [55]. As shown in this literature, the sulphur doping happens on hard DLC surface (hardness > 50 GPa) and the existence of H in a-C:H can prevent chemical mixing of sulphur into coatings.

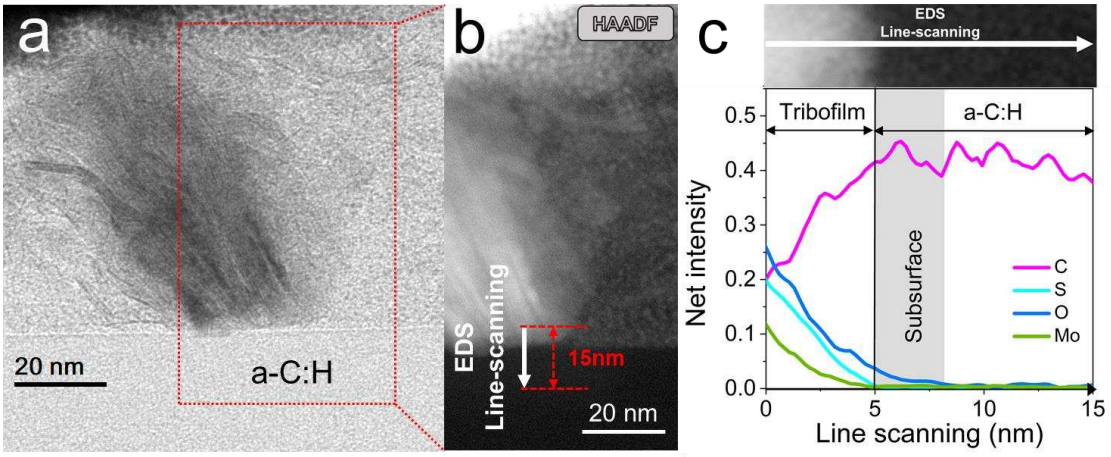

Figure 8. (a) HRTEM image showing the tribofilms after tribo-test (1 N, 140 mins). (b) HAADF image of selected area in (a). (c) EDS line-scanning results showing the elements distribution (C, Mo, O, and S) along the direction as marked in (b).

Based on this proposed mechanism, the following strategies of inhibiting the MoDTC-induced wear acceleration on a-C:H can be given: (a) The catalytic effect of molybdenum oxides in the oxidation of a-C:H can be eliminated by adding additives which are prone to react with molybdenum oxides. In the previous studies [10,56], it has been demonstrated that zinc dialkyldithiophosphate (ZDDP) can prevent the wear acceleration of MoDTC on a-C:H. This is because ZDDP will degrade into zinc phosphate in the friction process and phosphate anion (PO_4^{3-}) as a hard base prefers to react with Mo^{6-} of MoO_3 (hard acid) to form Zn/Mo phosphate according to hard and soft acids and bases (HSAB) principle. (b) For limiting the carbon source, it is suggested to use base oils with low carbon content (e.g. silicone oil and base oil containing fluorine) or high anti-shear ability (base oil containing rigid molecular chains like ester bond and aromatic ring).

4. CONCLUSION

The evolution process of MoDTC-derived tribofilms formed on a-C:H coating surface was investigated by combination of Raman-based profilometry, TEM and FFT. The obtained results confirmed that the remarkable deviations of Raman-based coating wear measurement were attributed to the tribofilm formation on the top surface of a-C:H due to their distinct optical properties compared with a-C:H. Formation of MoS_2 nano-sheet was observed in the initial stage, which was further converted into nano-MoC via carburization reaction under the impact of shear forces. In combination with previous studies about MoDTC-derived tribofilms, MoDTC-induced wear process on a-C:H/steel contact could be divided into two stages. In the first stage, wear acceleration was attributed to the catalytic effect of molybdenum oxides (accompaniment of MoS_2 derived from MoDTC) in the oxidation of a-C:H and easy-shear capability of oxidation layers. While for the second stage, the tribo-induced MoS_2 carburization into hard MoC led to abrasive wear, dominating the wear acceleration process. Based on this proposed mechanism, inhibiting strategies for the detrimental effect of MoDTC were also provided. The findings of this study may open a new pathway for detecting tribofilm composition formed on coating surface and clarifying its relation to coating wear behaviors which can help gain fundamental insights into wear mechanisms of a broad range of additives and coatings, and thus benefit the development and optimization of effective solid-liquid lubricating system.

ASSOCIATED CONTENT

Supporting Information

The Supporting Information is available free of charge on the ACS Publications website.

3D optical microscopy images of samples with a-C:H coatings of different thickness deposited on Si wafers and the corresponding step height values; HRTEM image of cross-sectional morphology of the a-C:H surface with iridium and platinum layers; Optical image

of line-scanning trace of Raman spectroscopy across the wear track; Schematic illustration of Raman-based coating thickness quantification method under dry friction; Optical parameters of a-C:H coatings deposited on glass plates; Friction behavior of a-C:H film under oil lubrication (PAO + 0.8 wt.% MoDTC) and 3D images of wear scars obtained by optical profilometer after depositing iridium layers; Evolution of width and depth of wear scars with test time under oil lubrication.

AUTHOR INFORMATION

Corresponding Author

Email: mnnx@leeds.ac.uk (Nan Xu) and A.Morina@leeds.ac.uk (Ardian Morina)

Author Contributions

Nan Xu: Designed the methodology, tribological experiments, coatings deposition, spectroscopy analyses, interpretation of the results, writing the original draft. **Chun Wang**: Supervision and contributed to writing the manuscript. **Liuquan Yang**: Supervision and contributed to writing the manuscript. **Gin Jose**: Supervision and contributed to writing the manuscript. **Ardian Morina**: Conceived the research, supervision, methodology, interpretation of the results and contributed to writing the manuscript. All authors discussed the results and approved the final version of the manuscript.

Notes

The authors declare no competing financial interest.

ACKNOWLEDGEMENTS

The authors thank the helpful assistance for FIB and TEM tests by Mr. John Harrington, Mrs. Zebeada Aslam, and Mr. Stuart Micklethwaite from Leeds Electron Microscopy and Spectroscopy Centre (LEMAS), University of Leeds. The authors are grateful for facility

access support by the Engineering and Physical Sciences Research Council (EPSRC, Grant no. EP/R02524X/1) in the UK. This work is partly supported by the Engineering and Physical Sciences Research Council (grant number EP/R001766/1) as a part of 'Friction: The Tribology Enigma' (www.friction.org.uk), a collaborative Programme Grant between the universities of Leeds and Sheffield.

REFERENCES

(1) Fan, X.; Xue, Q.; Wang, L. Carbon-Based Solid-Liquid Lubricating Coatings for Space Applications-A Review. *Friction* **2015**, *3* (3), 191–207.

(2) Fan, X.; Wang, L.; Li, W.; Wan, S. Improving Tribological Properties of Multialkylated Cyclopentanes under Simulated Space Environment: Two Feasible Approaches. *ACS Appl. Mater. Interfaces* **2015**, *7* (26), 14359–14368.

(3) Zhu, S.; Yu, Y.; Cheng, J.; Qiao, Z.; Yang, J.; Liu, W. Solid/Liquid Lubrication Behavior of Nickel Aluminum-Silver Alloy under Seawater Condition. *Wear* **2019**, *420–421*, 9–16.

(4) Kosarieh, S.; Morina, A.; Lainé, E.; Flemming, J.; Neville, A. The Effect of MoDTC-Type Friction Modifier on the Wear Performance of a Hydrogenated DLC Coating. *Wear* **2013**, *302* (1–2), 890–898.

(5) Zou, Y. S.; Wu, Y. F.; Yang, H.; Cang, K.; Song, G. H.; Li, Z. X.; Zhou, K. The Microstructure, Mechanical and Friction Properties of Protective Diamond like Carbon Films on Magnesium Alloy. *Applied Surface Science* **2011**, *258* (4), 1624–1629.

(6) Haque, T.; Morina, A.; Neville, A. Influence of Friction Modifier and Antiwear Additives on the Tribological Performance of a Non-Hydrogenated DLC Coating. *Surface and Coatings Technology* **2010**, *204* (24), 4001–4011.

(7) Morina, A.; Zhao, H.; Mosselmans, J. F. W. In-Situ Reflection-XANES Study of ZDDP and MoDTC Lubricant Films Formed on Steel and Diamond like Carbon (DLC) Surfaces. *Applied Surface Science* **2014**, *297*, 167–175.

(8) Erdemir, A.; Ramirez, G.; Eryilmaz, O. L.; Narayanan, B.; Liao, Y.; Kamath, G.; Sankaranarayanan, S. K. R. S. Carbon-Based Tribofilms from Lubricating Oils. *Nature* **2016**, *536* (7614), 67–71.

(9) Wu, H.; Khan, A. M.; Johnson, B.; Sasikumar, K.; Chung, Y.-W.; Wang, Q. J. Formation and Nature of Carbon-Containing Tribofilms. *ACS Appl. Mater. Interfaces* **2019**, *11* (17), 16139–16146.

(10) Morina, A.; Neville, A.; Priest, M.; Green, J. H. ZDDP and MoDTC Interactions and Their Effect on Tribological Performance – Tribofilm Characteristics and Its Evolution. *Tribol Lett* **2006**, *24* (3), 243–256.

(11) Vengudusamy, B.; Green, J. H.; Lamb, G. D.; Spikes, H. A. Tribological Properties of Tribofilms Formed from ZDDP in DLC/DLC and DLC/Steel Contacts. *Tribology International* **2011**, *44* (2), 165–174.

(12) Abdullah Tasdemir, H.; Wakayama, M.; Tokoroyama, T.; Kousaka, H.; Umehara, N.; Mabuchi, Y.; Higuchi, T. The Effect of Oil Temperature and Additive Concentration on the Wear of Non-Hydrogenated DLC Coating. *Tribology International* **2014**, *77*, 65–71.

(13) De Feo, M.; De Barros Bouchet, M. I.; Minfray, C.; Esnouf, C.; Le Mogne, Th.; Meunier, F.; Yang, L.; Thiebaut, B.; Pavan, S.; Martin, J. M. Formation of Interfacial Molybdenum Carbide for DLC Lubricated by MoDTC: Origin of Wear Mechanism. *Wear* **2017**, *370–371*, 17–28.

(14) De Feo, M.; De Barros Bouchet, M. I.; Minfray, C.; Le Mogne, Th.; Meunier, F.; Yang, L.; Thiebaut, B.; Martin, J. M. MoDTC Lubrication of DLC-Involving Contacts. Impact of MoDTC Degradation. *Wear* **2016**, *348–349*, 116–125.

(15) Okubo, H.; Sasaki, S. In Situ Raman Observation of Structural Transformation of Diamond-like Carbon Films Lubricated with MoDTC Solution: Mechanism of Wear

Acceleration of DLC Films Lubricated with MoDTC Solution. *Tribology International* **2017**, *113*, 399–410.

(16) Okubo, H.; Tadokoro, C.; Sumi, T.; Tanaka, N.; Sasaki, S. Wear Acceleration Mechanism of Diamond-like Carbon (DLC) Films Lubricated with MoDTC Solution: Roles of Tribofilm Formation and Structural Transformation in Wear Acceleration of DLC Films Lubricated with MoDTC Solution. *Tribology International* **2019**, *133*, 271–287.

(17) Khaemba, D. N.; Neville, A.; Morina, A. A Methodology for Raman Characterisation of MoDTC Tribofilms and Its Application in Investigating the Influence of Surface Chemistry on Friction Performance of MoDTC Lubricants. *Tribol Lett* **2015**, *59* (3), 38.

(18) Khaemba, D. N.; Neville, A.; Morina, A. A Methodology for Raman Characterisation of MoDTC Tribofilms and Its Application in Investigating the Influence of Surface Chemistry on Friction Performance of MoDTC Lubricants. *Tribol Lett* **2015**, *59* (3), 38.

(19) Xu, D.; Wang, C.; Espejo, C.; Wang, J.; Neville, A.; Morina, A. Understanding the Friction Reduction Mechanism Based on Molybdenum Disulfide Tribofilm Formation and Removal. *Langmuir* **2018**, *34* (45), 13523–13533.

(20) Xu, N.; Wang, C.; Yang, L.; Barimah, E. K.; Jose, G.; Neville, A.; Morina, A. Nano-Scale Coating Wear Measurement by Introducing Raman-Sensing Underlayer. *Journal of Materials Science & Technology* **2022**, *96*, 285–294.

(21) Chu, P. K.; Li, L. Characterization of Amorphous and Nanocrystalline Carbon Films. *Materials Chemistry and Physics* **2006**, *96* (2–3), 253–277.

(22) Kosarieh, S.; Morina, A.; Flemming, J.; Lainé, E.; Neville, A. Wear Mechanisms of Hydrogenated DLC in Oils Containing MoDTC. *Tribol Lett* **2016**, *64* (1), 4.

(23) Al-Jeboori, Y.; Kosarieh, S.; Morina, A.; Neville, A. Investigation of Pure Sliding and Sliding/Rolling Contacts in a DLC/Cast Iron System When Lubricated in Oils Containing MoDTC-Type Friction Modifier. *Tribology International* **2018**, *122*, 23–37.

(24) De Barros'Bouchet, M. I.; Martin, J. M.; Le-Mogne, T.; Vacher, B. Boundary Lubrication Mechanisms of Carbon Coatings by MoDTC and ZDDP Additives. *Tribology International* **2005**, *38* (3), 257–264.

(25) Topolovec-Miklozic, K.; Lockwood, F.; Spikes, H. Behaviour of Boundary Lubricating Additives on DLC Coatings. *Wear* **2008**, *265* (11–12), 1893–1901.

(26) Morina, A.; Neville, A.; Priest, M.; Green, J. H. ZDDP and MoDTC Interactions in Boundary Lubrication—The Effect of Temperature and ZDDP/MoDTC Ratio. *Tribology International* **2006**, *39* (12), 1545–1557.

(27) Neville, A.; Morina, A.; Haque, T.; Voong, M. Compatibility between Tribological Surfaces and Lubricant Additives—How Friction and Wear Reduction Can Be Controlled by Surface/Lube Synergies. *Tribology International* **2007**, *40* (10–12), 1680–1695.

(28) Gesheva, K.; Szekeres, A.; Ivanova, T. Optical Properties of Chemical Vapor Deposited Thin Films of Molybdenum and Tungsten Based Metal Oxides. *Solar Energy Materials and Solar Cells* **2003**, *76* (4), 563–576.

(29) Sian, T. S.; Reddy, G. B. Optical, Structural and Photoelectron Spectroscopic Studies on Amorphous and Crystalline Molybdenum Oxide Thin Films. *Solar Energy Materials and Solar Cells* **2004**, *82* (3), 375–386.

(30) Al-Kuhaili, M. F.; Saleem, M.; Durrani, S. M. A. Optical Properties of Iron Oxide (α-Fe2O3) Thin Films Deposited by the Reactive Evaporation of Iron. *Journal of Alloys and Compounds* **2012**, *521*, 178–182.

(31) Wang, H.; Shen, J.; Qian, J. Magneto-Optic Faraday Rotation of Sputtered γ-Fe2O3 Film. *Journal of Magnetism and Magnetic Materials* **1988**, *73* (1), 103–105.

(32) De Temmerman, G.; Ley, M.; Boudaden, J.; Oelhafen, P. Study of Optical Properties of MoxC1−x Films. *Journal of Nuclear Materials* **2005**, *337–339*, 956–959.

(33) Feng, W.; Wang, R.; Zhou, Y.; Ding, L.; Gao, X.; Zhou, B.; Hu, P.; Chen, Y. Ultrathin Molybdenum Carbide MXene with Fast Biodegradability for Highly Efficient Theory-Oriented Photonic Tumor Hyperthermia. *Adv. Funct. Mater.* **2019**, *29* (22), 1901942.

(34) Dashora, A.; Ahuja, U.; Venugopalan, K. Electronic and Optical Properties of MoS2 (0001) Thin Films: Feasibility for Solar Cells. *Computational Materials Science* **2013**, *69*, 216–221.

(35) Min, Y.; He, G.; Xu, Q.; Chen, Y. Dual-Functional MoS2 Sheet-Modified CdS Branch-like Heterostructures with Enhanced Photostability and Photocatalytic Activity. *J. Mater. Chem. A* **2014**, *2* (8), 2578-2584.

(36) Lee, C.; Yan, H.; Brus, L. E.; Heinz, T. F.; Hone, J.; Ryu, S. Anomalous Lattice Vibrations of Single- and Few-Layer MoS_2. *ACS Nano* **2010**, *4* (5), 2695–2700.

(37) Li, X.; Zhang, J.; Wang, R.; Huang, H.; Xie, C.; Li, Z.; Li, J.; Niu, C. In Situ Synthesis of Carbon Nanotube Hybrids with Alternate MoC and MoS_2 to Enhance the Electrochemical Activities of MoS_2. *Nano Lett.* **2015**, *15* (8), 5268–5272.

(38) Spikes, H. Stress-Augmented Thermal Activation: Tribology Feels the Force. *Friction* **2018**, *6* (1), 1–31.

(39) Yin, X.; Wu, F.; Chen, X.; Xu, J.; Wu, P.; Li, J.; Zhang, C.; Luo, J. Graphene-Induced Reconstruction of the Sliding Interface Assisting the Improved Lubricity of Various Tribo-Couples. *Materials & Design* **2020**, *191*, 108661.

(40) Xu, J.; Luo, T.; Chen, X.; Zhang, C.; Luo, J. Nanostructured Tribolayer-Dependent Lubricity of Graphene and Modified Graphene Nanoflakes on Sliding Steel Surfaces in Humid Air. *Tribology International* **2020**, *145*, 106203.

(41) Zhao, J.; Huang, Y.; Li, Y.; Gao, T.; Dou, Z.; Mao, J.; Wang, H.; He, Y.; Li, S.; Luo, J. Superhigh-Exfoliation Graphene with a Unique Two-Dimensional (2D) Microstructure for Lubrication Application. *Applied Surface Science* **2020**, *513*, 145608.

(42) Xu, X.; Xu, Z.; Sun, J.; Tang, G.; Su, F. In Situ Synthesizing Carbon-Based Film by Tribo-Induced Catalytic Degradation of Poly-α-Olefin Oil for Reducing Friction and Wear. *Langmuir* **2020**, *36* (35), 10555–10564.

(43) Argibay, N.; Babuska, T. F.; Curry, J. F.; Dugger, M. T.; Lu, P.; Adams, D. P.; Nation, B. L.; Doyle, B. L.; Pham, M.; Pimentel, A.; Mowry, C.; Hinkle, A. R.; Chandross, M. In-Situ Tribochemical Formation of Self-Lubricating Diamond-like Carbon Films. *Carbon* **2018**, *138*, 61–68.

(44) Rusanov, A.; Nevshupa, R.; Fontaine, J.; Martin, J.-M.; Le Mogne, T.; Elinson, V.; Lyamin, A.; Roman, E. Probing the Tribochemical Degradation of Hydrogenated Amorphous Carbon Using Mechanically Stimulated Gas Emission Spectroscopy. *Carbon* **2015**, *81*, 788–799.

(45) Ji, L.; Wang, J.; Teng, X.; Dong, H.; He, X.; Chen, Z. N,P-Doped Molybdenum Carbide Nanofibers for Efficient Hydrogen Production. *ACS Appl. Mater. Interfaces* **2018**, *10* (17), 14632–14640.

(46) Lv, C.; Huang, Z.; Yang, Q.; Wei, G.; Chen, Z.; Humphrey, M. G.; Zhang, C. Ultrafast Synthesis of Molybdenum Carbide Nanoparticles for Efficient Hydrogen Generation. *J. Mater. Chem. A* **2017**, *5* (43), 22805–22812.

(47) Alazizi, A.; Draskovics, A.; Ramirez, G.; Erdemir, A.; Kim, S. H. Tribochemistry of Carbon Films in Oxygen and Humid Environments: Oxidative Wear and Galvanic Corrosion. *Langmuir* **2016**, *32* (8), 1996–2004.

(48) Shi, J.; Gong, Z.; Wang, C.; Zhang, B.; Zhang, J. Tribological Properties of Hydrogenated Amorphous Carbon Films in Different Atmospheres. *Diamond and Related Materials* **2017**, *77*, 84–91.

(49) Afsharpour, M.; Mahjoub, A.; Amini, M. M. A Nano-Hybrid of Molybdenum Oxide Intercalated by Dithiocarbamate as an Oxidation Catalyst. *J Inorg Organomet Polym* **2008**, *18* (4), 472–476.

(50) Wang, D.-Y.; Chang, C.-L.; Ho, W.-Y. Oxidation Behavior of Diamond-like Carbon Films. *Surface and Coatings Technology* **1999**, *120–121*, 138–144.

(51) Al-Azizi, A. A.; Eryilmaz, O.; Erdemir, A.; Kim, S. H. Surface Structure of Hydrogenated Diamond-like Carbon: Origin of Run-In Behavior Prior to Superlubricious Interfacial Shear. *Langmuir* **2015**, *31* (5), 1711–1721.

(52) Fontaine, J.; Le Mogne, T.; Loubet, J. L.; Belin, M. Achieving Superlow Friction with Hydrogenated Amorphous Carbon: Some Key Requirements. *Thin Solid Films* **2005**, *482* (1–2), 99–108.

(53) Yang, M.; Marino, M. J.; Bojan, V. J.; Eryilmaz, O. L.; Erdemir, A.; Kim, S. H. Quantification of Oxygenated Species on a Diamond-like Carbon (DLC) Surface. *Applied Surface Science* **2011**, *257* (17), 7633–7638.

(54) Shi, J.; Gong, Z.; Wang, Y.; Gao, K.; Zhang, J. Friction and Wear of Hydrogenated and Hydrogen-Free Diamond-like Carbon Films: Relative Humidity Dependent Character. *Applied Surface Science* **2017**, *422*, 147–154.

(55) Salinas Ruiz, V. R.; Kuwahara, T.; Galipaud, J.; Masenelli-Varlot, K.; Hassine, M. B.; Héau, C.; Stoll, M.; Mayrhofer, L.; Moras, G.; Martin, J. M.; Moseler, M.; de Barros Bouchet, M.-I. Interplay of Mechanics and Chemistry Governs Wear of Diamond-like Carbon Coatings Interacting with ZDDP-Additivated Lubricants. Nat Commun 2021, 12 (1), 4550.

(56) Martin, J.; Grossiord, C.; Varlot, K.; Vacher, B.; Igarashi, J. Synergistic effects in binary systems of lubricant additives: a chemical hardness approach. *Tribology Letters* **2000**, *8* (4), 193–201.

TOC

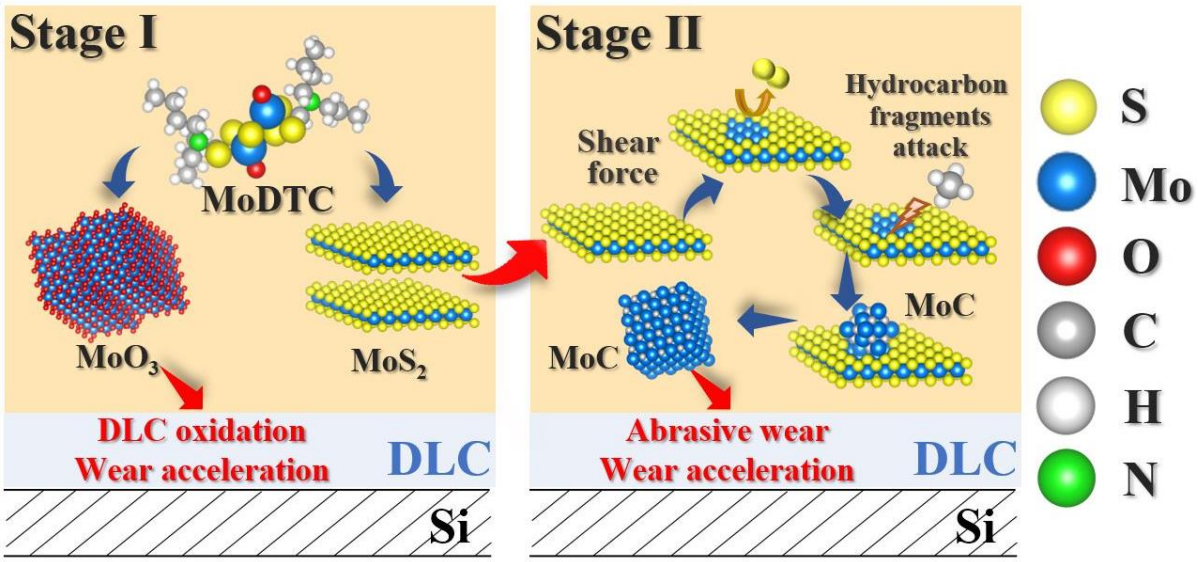
Stage I
MoDTC
MoO_3
MoS_2
DLC oxidation
Wear acceleration
DLC
Si
Stage II
Shear force
Hydrocarbon fragments attack
MoC
MoC
Abrasive wear
Wear acceleration
DLC
Si
S
Mo
O
C
H
N